Electronic Supplementary Material (ESI) for Materials Advances.

Supplementary Information

Fabrication of Highly Efficient Encapsulated SnO_2@Alginate Beads as Regenerative Nanosorbents for Anionic Dye Pollutants Removal from Aqueous Solution

Shikha Jyoti Borah[1], Akanksha Gupta[2], Kashyap Kumar Dubey[3], Vinod Kumar*[1]

[1]Special Centre for Nano Science, Jawaharlal Nehru University, Delhi-110067, India; [2]Department of Science and Technology, Delhi-110016, India; [3]School of Biotechnology, Jawaharlal Nehru University, Delhi-110067, India.

S1: Adsorption Efficiency

S2: Adsorption Kinetics

S3: Adsorption Isotherms

S4: Calculation for Sn concentration in treater water

Table S1: Adsorption isotherm parameters obtained using Langmuir, Freundlich and Temkin model

Figure S1: Moving anti-clockwise, 1,2,3 and 4 depicts synthesized SnO_2 NPs, SnO_2 NPs after adsorption of CR dye, completely dried SnO_2@SA beads and completely dried SnO_2@SA beads after adsorption, respectively.

Figure S2: From L to R, pure SA beads, 0.2% SnO_2@SA beads and 0.2% SnO_2@SA beads after adsorption of CR dye.

Figure S3: XRD obtained for SnO_2@SA beads (a) before and (b) after adsorption of 5 μM CR from its aqueous solution.

Figure S4: SEM images of (a) various sizes of spherically shaped SnO_2 NPs; (b), (c) and (d) 0.2% SnO_2@SA beads at various magnifications.

Figure S5: (a) UV-Vis plot for different concentrations of CR dye (5- 60 μM); (b) Linear fit analysis and (c) Image of the various CR concentrations used in this study.

Figure S6: Adsorption of 5 μM CR dye using (a) 0.1 g SnO_2 NPs and (b) 0.5% SnO_2@SA beads

Figure S7: 0.1% SnO_2@SA beads before and after 10 min adsorption

Figure S8: 0.2% SnO_2@SA beads before and after 10 min adsorption

Figure S9: Adsorption of 5 μM CR using 0.5% SnO_2@SA beads within 5 min

Figure S10: MeOH used as an elluent for regenerative studies pale red color observed after being in contact with 0.2% SnO_2@SA beads for 2 min with continuous stirring

Video S1: Video demonstrating the adsorption of CR by SnO_2 NPs. Within 1 min of contact time rapid adsorption results in change in color from light red to nearly grayish white color.

Video S2: Video demonstrating the adsorption of CR by 0.5% SnO_2@SA beads. Within the first min of contact, rapid adsorption results in change in color from light red to nearly transparent solution.

S1: Adsorption Efficiency

The removal efficiency (η) has been calculated using Equation (S1), where C_o and C_t are concentrations at t=0 and at time t, respectively[1,2].

$$\eta = \frac{C_0 - C_t}{C_0} \times 100$$ Equation S1

S2: Adsorption Kinetics

The PFO[3] kinetic model is expressed as:

$$\ln (q_e - q_t) = \ln (q_e) - k_1 t,$$ Equation S2

where k_1 (min^{-1}) refers to the equilibrium rate constant; q_e (mg/g) and q_t (mg/g) indicate the amount of dye adsorbed at equilibrium and time t, respectively. The slope and intercept obtained from the plot of ln (q_e-q_t) versus t were used to determine the values of k_1 and q_e, respectively.

Contrastingly, the pseudo-second-order (PSO)[4] kinetic model follows the equation:

$$\frac{t}{q_t} = \frac{1}{k_2 q_e^2} + \left(\frac{1}{q_e}\right) t,$$ Equation S3

where k_2 (g mg^{-1} min^{-1}) refers to the PSO rate constant. The plot of $\frac{t}{q_t}$ versus t is used to determine the values of k_2 and q_e.

Additional investigations to determine the probabilities of IPD resistance affecting the adsorption of CR on SnO_2 were carried out by using IPD[5,6] model, which follows:

$$q_t = k_p t^{1/2} + C,$$ Equation S4

where k_p (mg g^{-1} $min^{-1/2}$) is the IPD rate constant and C (mg/g) is the intercept. The slope from the linear plot of q_t versus $t^{1/2}$, is used to determine the values of k_p and q_e.

S3. Adsorption Isotherms

The Langmuir isotherm predicts that monolayer adsorption originates at binding sites with homogeneous energy levels, independent of interactions between adsorbed molecules and the transfer of adsorbed molecule onto the adsorption surface[7]. The Langmuir equation can be expressed as:

$$\frac{C_e}{q_e} = \frac{1}{k_1 q_m} + \frac{1}{q_m} C_e,$$ Equation S5

where q_e, C_e, k_1, q_m are adsorption capacity at equilibrium (mg/g), equilibrium concentration (mg/L), constant related to free energy of adsorption (L/mg) and maximum adsorption capacity at monolayer coverage (mg/g), respectively.

The favorability of the adsorption isotherm was further determined by evaluating the dimensionless separation factor (R_L), using the equation[7,8]

$$R_L = \frac{1}{1 + k_1 C_0}$$ Equation S6

The Freundlich isotherm holds true for non-ideal sorption on heterogeneous surfaces as well as multilayer sorption[9]. It is represented as:

$$lnq_e = lnk_f - \frac{1}{n} lnC_e,$$ Equation S7

where k_f and n are the Freundlich constants of the system. The reaction is favorable when 0< $1/n$<1, but reaction is unfavorable if $\frac{1}{n} > 1$.

Temkin isotherm is generally used for heterogeneous systems or non-uniform distribution of sorption heat[10]. It is represented as

$$q_e = \frac{RT}{b} lnK_t + \frac{RT}{b} lnC_e,$$ Equation S7

where K_t is the equilibrium binding constant, b is related to the adsorption heat, R is universal gas constant and T is temperature.

S4: Calculation for Sn concentration in treated water

Molecular weight of SnO_2 = 151 g and atomic weight of Sn = 118 g

151 g of SnO_2 has 118 g of Sn, then 0.5 g of SnO_2 contains, $\frac{0.5 \times 118}{151} = 0.3940\ g = 394\ mg$

394 mg of Sn is used to prepare SnO_2@SA beads, which are added to 100 mL of CR dye aqueous solution. So, 394mg/100 mL or 3940 mg/L of Sn (encapsulated within beads) is used to treat CR dye aqueous solution.

Detected Sn levels in treated water = 7.729 ppb or 0.007729 mg/L.

Thus, percentage of Sn present in CR after treatment = $\frac{0.007729}{3940} \times 100 = 0.0002\ \%$

Table S1 Adsorption isotherm parameters obtained using Langmuir, Freundlich and Temkin model

Langmuir Model	
q_m (mg/g)	961.54
R^2	0.9998
k_L	8.8135
R_L	0.000113
Freundlich Model	
R^2	0.9177
1/n	0.0083
k_f	20.025
Temkin Model	
R^2	0.9178

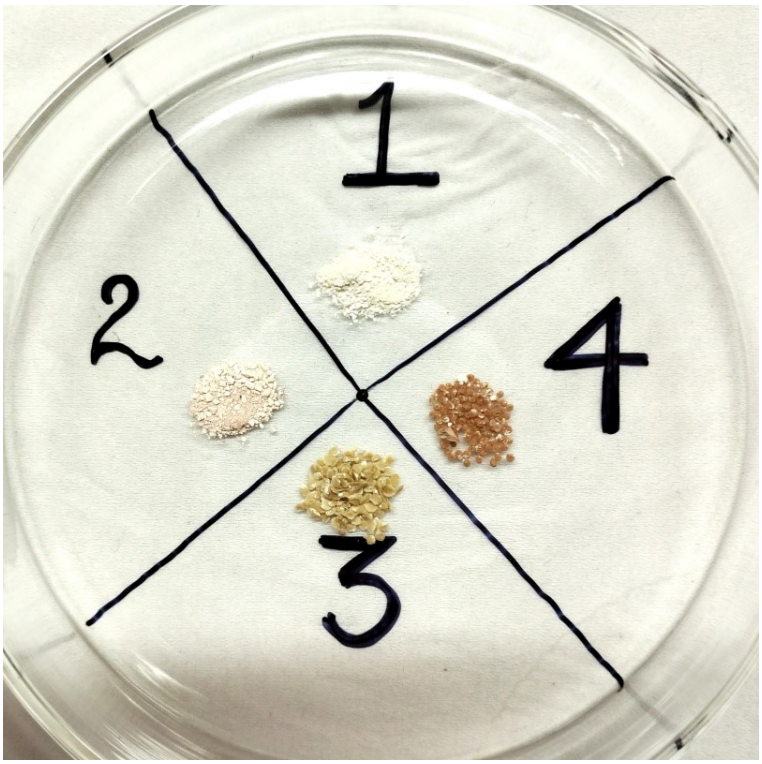

Fig. S1. Moving anti-clockwise, 1,2,3 and 4 depicts synthesized SnO_2 NPs, 0.1 g SnO_2 NPs after adsorption of CR dye, completely dried 0.5% SnO_2@SA beads and completely dried 0.5 % SnO_2@SA beads after adsorption, respectively.

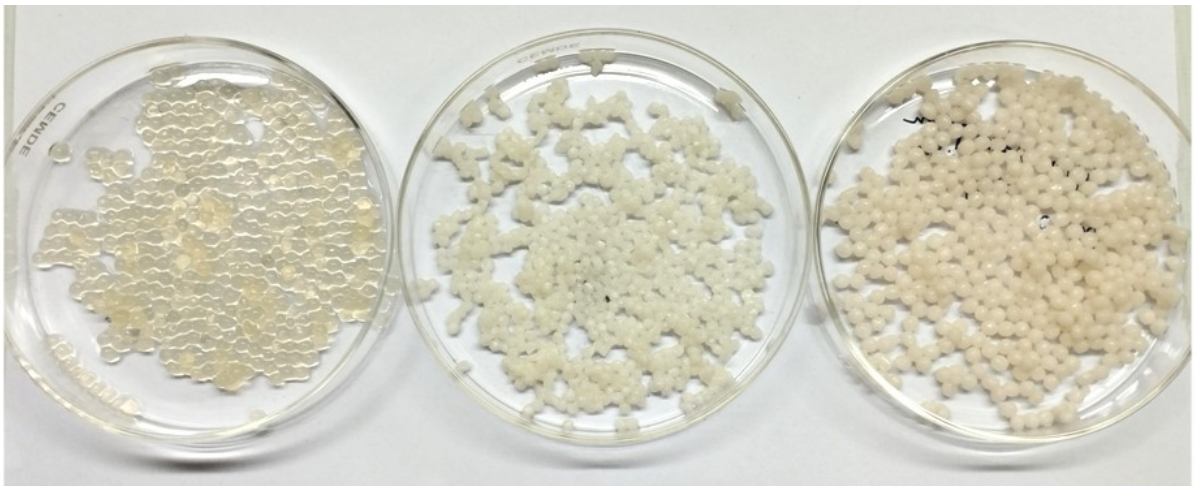

Fig. S2. From L to R, pure SA beads, 0.2% SnO_2@SA beads and 0.2% SnO_2@SA beads after adsorption of CR dye

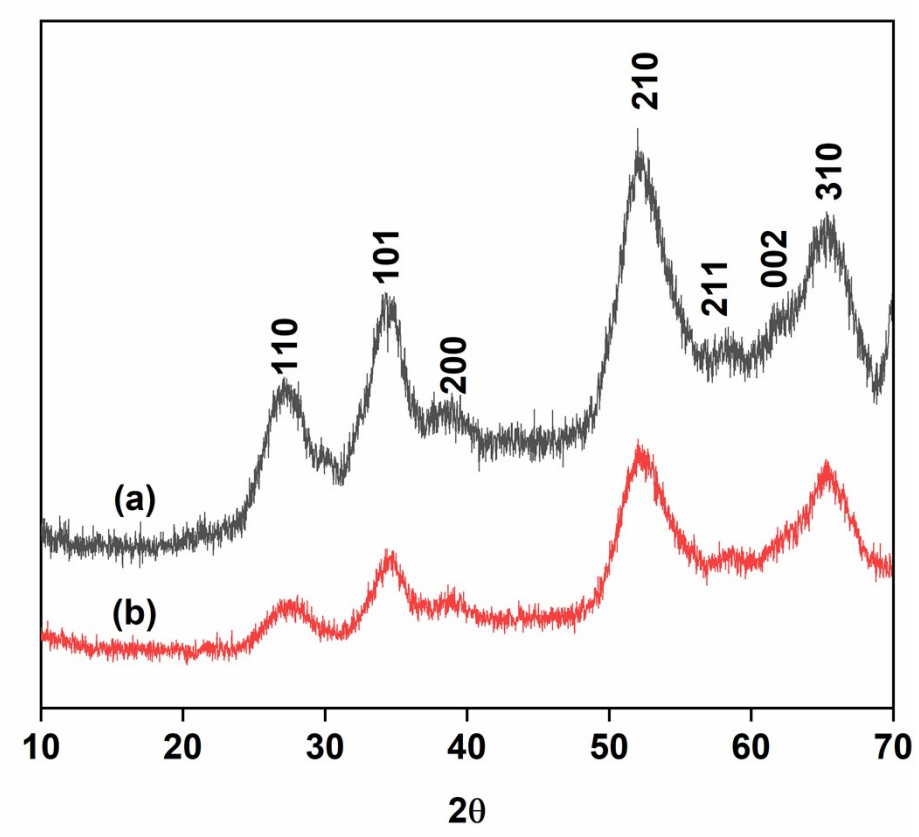

Fig. S3. XRD obtained for SnO_2@SA beads (a) before and (b) after adsorption of 5 μM CR from its aqueous solution.

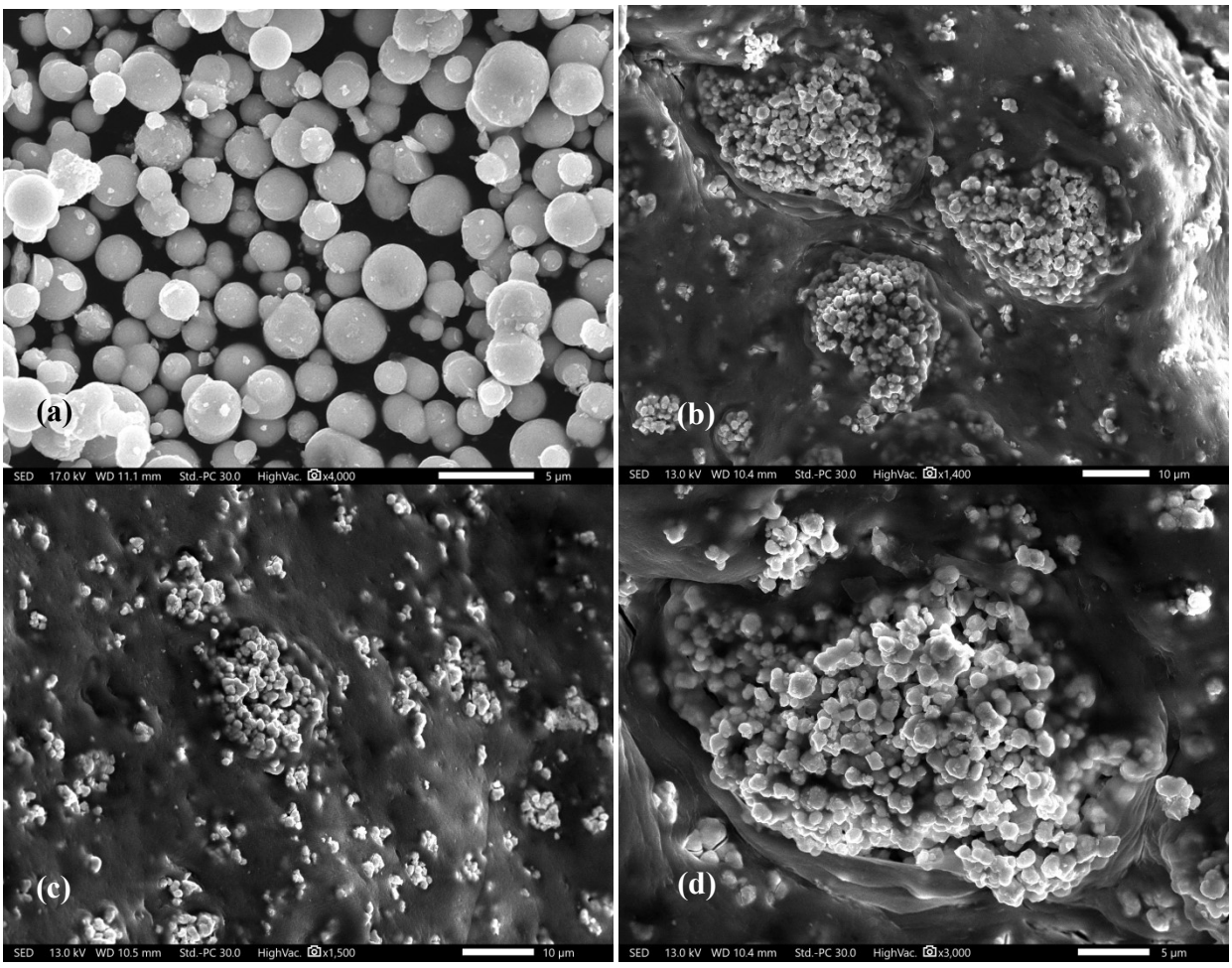

Fig. S4. SEM images of (a) various sizes of spherically shaped SnO_2 NPs; (b), (c) and (d) 0.2% SnO_2@SA beads at various magnifications

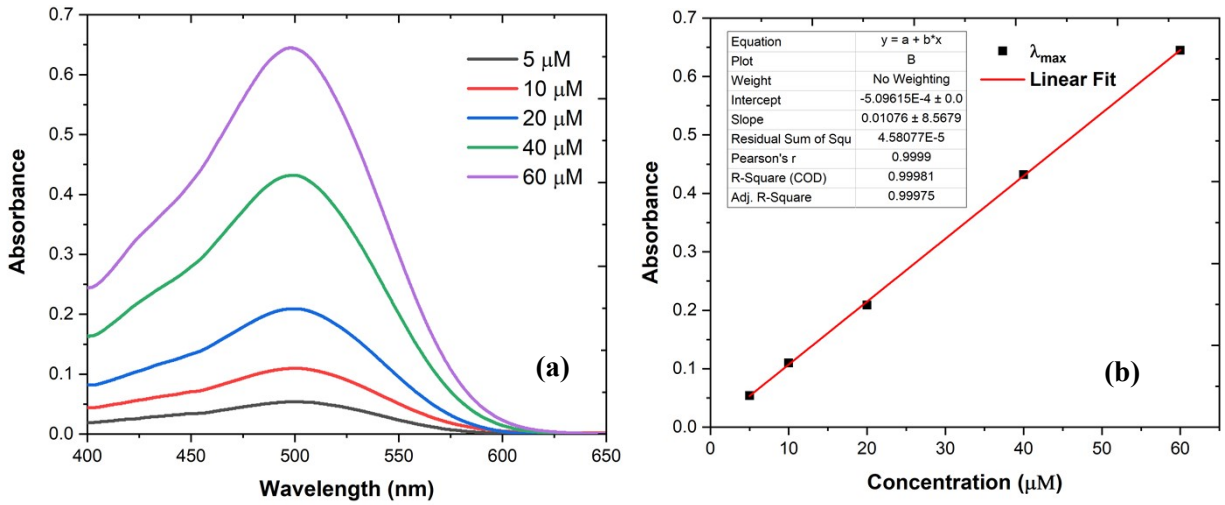

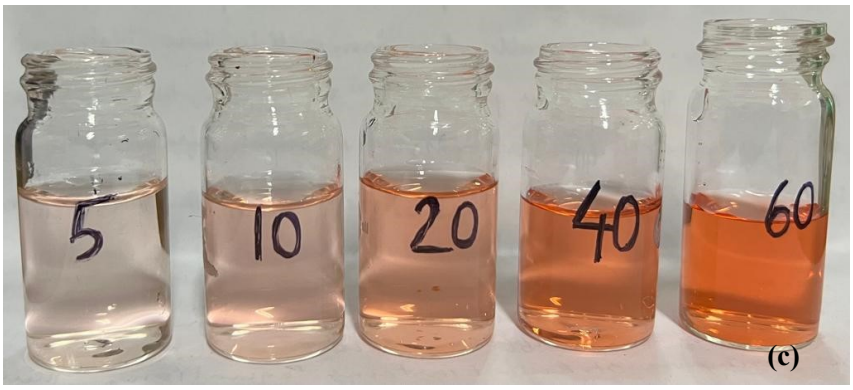

Fig. S5. (a) UV-Vis plot for different concentrations of CR dye (5- 60 µM); (b) Linear fit analysis and (c) Image of the various CR concentrations used in this study

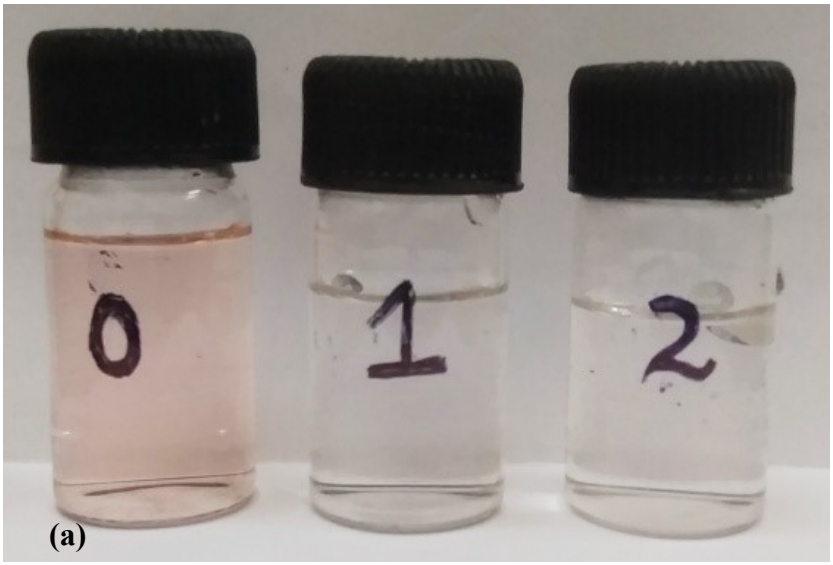

Fig. S6. Adsorption of 5 µM CR dye using (a) powdered 0.1 g SnO_2 NPs and (b) 0.5% SnO_2@SA beads

Fig. S7. 0.1% SnO_2@SA beads before and after 10 min adsorption

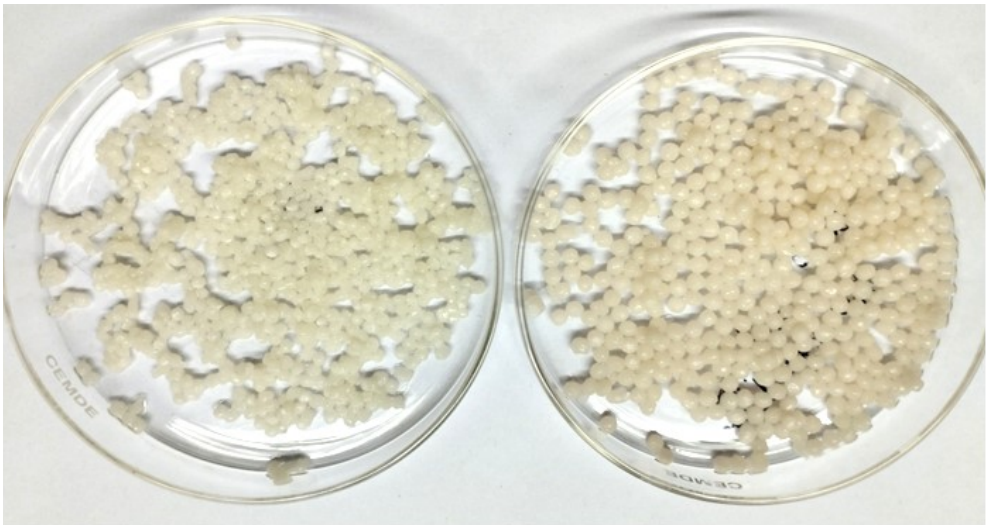

Fig. S8. 0.2% SnO_2@SA beads before and after 10 min adsorption

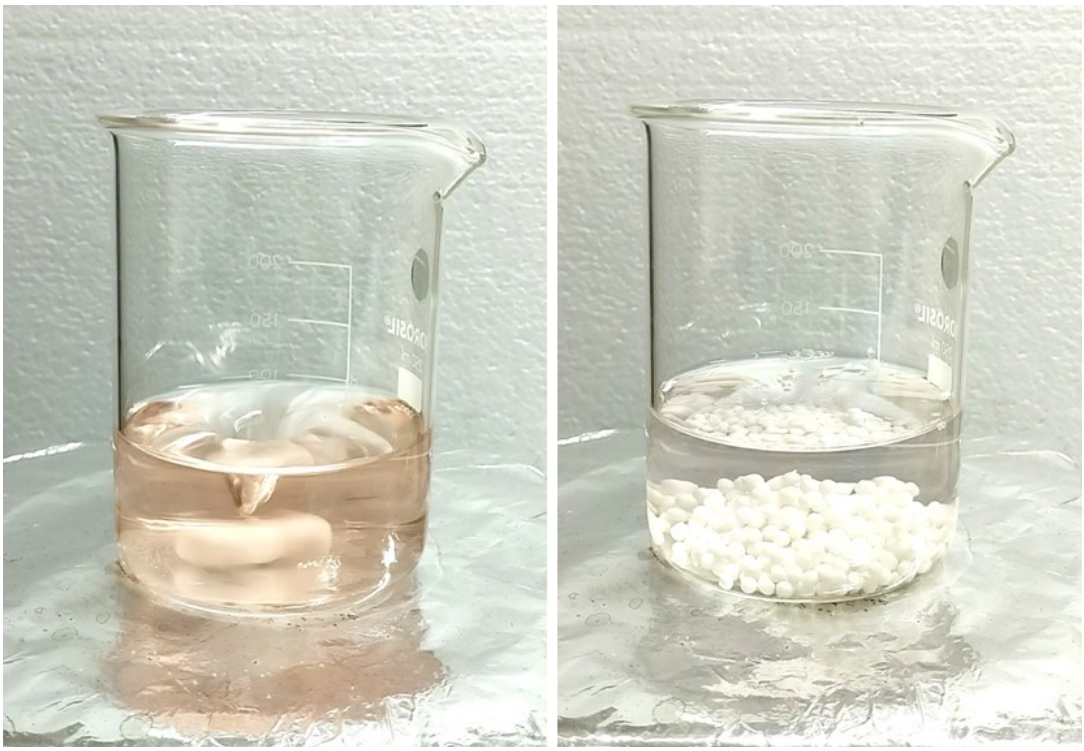

Fig. S9. Adsorption of 5 µM CR using 0.5% SnO_2/SA beads within 2 min

Fig. S10. MeOH used as an elluent for regenerative studies pale red color observed after being in contact with 0.2% SnO_2@SA beads for 2 min with continuous stirring

References

1 M. Mohammadi Galangash, M. Mohaghegh Montazeri, A. Ghavidast and M. Shirzad-Siboni, Synthesis of carboxyl-functionalized magnetic nanoparticles for adsorption of malachite green from water: Kinetics and thermodynamics studies, *J. Chinese Chem. Soc.*, 2018, **65**, 940–950.

2 E. Abdelkader, L. Nadjia and V. Rose-Noëlle, Adsorption of Congo red azo dye on nanosized SnO2 derived from sol-gel method, *Int. J. Ind. Chem.*, 2016, **7**, 53–70.

3 S. Lagergren, Zur theorie der sogenannten adsorption geloster stoffe, *K. Sven. vetenskapsakademiens. Handl.*, 1898, **24**, 1–39.

4 Y.-S. Ho and G. McKay, Pseudo-second order model for sorption processes, *Process Biochem.*, 1999, **34**, 451–465.

5 W. J. Weber Jr and J. C. Morris, Kinetics of adsorption on carbon from solution, *J. Sanit. Eng. Div.*, 1963, **89**, 31–59.

6 S. Alam, B. Ullah, M. S. Khan, N. ur Rahman, L. Khan, L. A. Shah, I. Zekker, J. Burlakovs, A. Kallistova and N. Pimenov, Adsorption kinetics and isotherm study of basic red 5 on synthesized silica monolith particles, *Water*, 2021, **13**, 2803.

7 I. Langmuir, The adsorption of gases on plane surfaces of glass, mica and platinum., *J. Am. Chem. Soc.*, 1918, **40**, 1361–1403.

8 H. Jiang, Y. Cao, F. Zeng, Z. Xie and F. He, A Novel Fe_3O_4/Graphene Oxide Composite Prepared by Click Chemistry for High-Efficiency Removal of Congo Red from Water, *J. Nanomater.*, 2021, **2021**, 9716897.

9 H. M. F. Freundlich, Over the adsorption in solution, *J. Phys. chem*, 1906, **57**, 1100–1107.

10 R. Sips, On the structure of a catalyst surface. II, *J. Chem. Phys.*, 1950, **18**, 1024–1026.